A NEW SHEAR FORMULA FOR TAPERED BEAMLIKE SOLIDS UNDERGOING EVEN LARGE DISPLACEMENTS

G. Migliaccio[1*], G. Ruta[2], R. Barsotti[1], S. Bennati[1]

[1] Civil and Industrial Engineering, University of Pisa;
Gruppo Nazionale di Fisica Matematica, Pisa, Italy

[2] Structural and Geotechnical Engineering, University "La Sapienza";
Gruppo Nazionale di Fisica Matematica, Roma, Italy

*Corresponding author (email): giovanni.migliaccio.it@gmail.com

Abstract. *In many engineering applications it is often necessary to determine the flow of shear stresses in the cross-sections of beam-like bodies. Taking a cue from Jourawski's well-known formula, several scholars have proposed expressions for evaluating the shear stresses in non-prismatic linear elastic beams, where longitudinal variations in the size and shape of the cross-sections produces complex stress fields. In the present paper, a new shear formula, derived using a mechanical model developed in a previous work, is presented for tapered beams subject to even large displacements and small strains. Numerical examples and comparisons with results obtained using other formulas in the literature and non-linear 3D-FEM simulations show how the new formula constitutes an important generalization of the previous ones and is able to provide particularly accurate results.*

Keywords: shear flow, tapered beams, shear formula, large displacements.

1 INTRODUCTION

Performing structural analyses of beamlike elements often involves using approximate relations for the stress and strain fields to deal with their torsion and flexure. This is because it is quite difficult to find closed-form analytical solutions to the Saint-Venant problems of torsion and flexure for beam shapes of practical interest [1-4]. In particular, as far as application-oriented formulas for shear stresses are concerned, it is usual to adopt the approximate closed-form expression for the shear flow based on the formula introduced by Jourawski in 1856 [5].

However, Jourawski's formula only holds for prismatic beams and linear kinematics. No general closed-form expressions for the shear flow are available for non-prismatic beams with

non-linear kinematics: in tapered or pre-twisted beams couplings appear among bending, twisting and traction that are instead uncoupled in prismatic isotropic beams [6-8], and large displacements further complicate the derivation of closed-form formulas.

Several attempts to find Jourawski-like solutions for non-prismatic beams undergoing small displacements started in the early 20th century: see for example the studies by Slocum [9], Bleich [10], Pugsley and Weatherhead [11], and Saksena [12], in the first half of the 20th century, and, subsequently, those by Krahula [13], Russo and Garic [14], Cortinez [15], Taglialegne [16], Bertolini et al. [17], and Balduzzi et al. [18], among others (a short review of contributions of this kind will be presented in the following section).

Apart from the works proposing a shear formula, tapered elements were studied via other approaches as well. Hodges et al. [19-20], for instance, exploited Berdichevsky's variational asymptotic method (VAM) [21] to study thin tapered elements in plane stress and compared their results with those of the well-known linear elastic solutions of the infinite wedge [4,13]. Zappino et al. [22] used the Carrera Unified Formulation (CUF) to describe the behaviour of tapered box-beams for aerospace engineering applications and compared their results with those of commercial FEM tools. Other investigators used 1D or 3D finite element methods to study non-prismatic beamlike bodies, e.g. [23-25]. However, approaches of this kind are not discussed further in this paper (details can be found in the reviews by Paglietti and Carta [26-27], and Balduzzi et al. [6,28]), as our goal here is to propose an analytical shear formula that generalizes Jourawski's for non-prismatic beams.

In all the studies available in the literature, to the best of our knowledge, small displacements are assumed, the equilibrium of tapered beams with symmetric cross-sections is imposed in the reference configuration, and Navier's formula is assumed to hold for the normal stresses. The main novelty in the present contribution consists in abandoning all such assumptions: we study bi-tapered beams with fully deformable transverse cross-sections, susceptible to large displacements and small strains.

The paper is organised as follows. In section 2 we briefly review the main contributions addressing a shear formula for tapered beams. The main features of the adopted beam model are sketched out in section 3. The new shear formula we propose for bi-tapered beams, generalizing Jourawski's in the non-linear setting mentioned in the foregoing, is presented in section 4. Finally, numerical examples and comparisons with the results of nonlinear 3D-FEM simulations are shown in section 5.

2 A SHORT SURVEY OF SHEAR FORMULAS AFTER JOURAWSKI

Non-prismatic beamlike elements are widespread in engineering applications as they allow optimizing strength, stiffness, materials, and costs. Therefore, it is not surprising that several studies over the last century have addressed the development of engineering methods and formulas for their analysis and design. In particular, the difficulty of addressing flexure via closed-form solutions and the need for application-oriented formulas for predicting shear flow led to the adoption of approximate methods, as Jourawski did for the prismatic case.

As is well-known, Jourawski derived his formula as a tool for the design of bridges while he was engaged in the construction of the St. Petersburg-Moscow railroad (1844-1850). The bridges involved wooden beams of great depth, for which the assessment of shear stresses was of key importance. He successfully determined an average measure of the shear stresses by imposing equilibrium with the normal stresses due to the bending moment as given by Navier's formula [5], for cantilever beams with rectangular cross-sections loaded at the free-end and undergoing infinitesimal displacements.

Since the early 20th century many investigators have exploited a similar approach to derive a shear formula for evaluating the shear stresses in tapered beams; a scheme typical of the literature is shown in Figure 1.

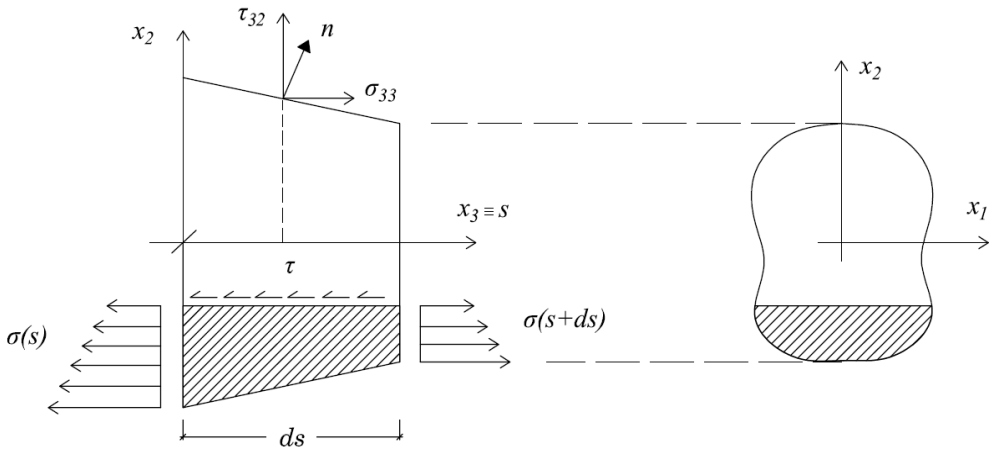

Figure 2: Lateral view of a tapered beamlike element (left) and its transverse cross-section (right)

In 1911, Slocum derived a shear formula for beams of arbitrary cross-sections [9], assuming Navier's formula for the normal stresses and accounting for the spanwise variation of the cross-sectional inertia. However, his formula yields zero shear stresses at the cross-section boundary (e.g. τ_{32} in Figure 2), hence making it impossible to fulfil the boundary condition on the lateral surface of non-prismatic beams in case of nil surface loads.

In 1932, Bleich followed a correct approach for beams of variable depth [10] to determine the mean shear stress τ_m (the subscript stands for *mittelwert*, i.e., 'mean value' in German) on any given cross-sectional chord, correctly accounting for the effects of transverse force, bending moment and axial force. However, he wrongly labelled as "max τ_m" the value of τ_m at the cross-section centroid, without considering that in the case of beams of variable depth τ_m may attain its maximum elsewhere. This fact caused improper uses of Bleich's formula in subsequent years, as also pointed out by Paglietti and Carta [26-27].

In the field of aerospace engineering, once again limiting their analysis to elements undergoing small displacements, Pugsley and Weatherhead in 1938 [11] investigated the failures of tail-plane spars in highly tapered regions. They focused on the errors arising from applying the conventional design methods of prismatic beams to tapered elements and, following Jourawski, proposed a shear formula for tapered beams that accounts for the bending moment and transverse force. In 1944, Saksena [12] used a similar approach to evaluate the shear stresses in elements for aerospace applications and provided examples for rectangular, circular and I-shaped cross-sections. Many other works in the second half of the 20th century addressed the problem via similar approaches [13-18, 28-33]. Krahula [13] compared the results of Singer's formula [32] with those of the linear elastic solutions for the infinite wedge [7]. In 1992, Russo and Garic [14] proposed a shear formula accounting for the effects of axial force, bending moment and transverse force, limiting their analysis to tapered beams with rectangular cross-sections in a linear setting. In 1994, Cortinez [15] discussed the study of Russo and Garic [14] and extended it to generic symmetric cross-sections. Recently, Taglialegne [16] and Bertolini et al. [17] proposed a similar formula for tapered beams with doubly symmetric cross-sections via the balance of a beam slice, assuming Navier's formula. The shear stresses in tapered thin-walled beams with symmetric cross-sections were evaluated via a Jourawski-like approach by Balduzzi et al. [18] as well. Further details on critical issues, deficiencies of engineering methods, and accuracy of approaches developed so far for tapered thin-walled beams can be found in the reviews by Balduzzi et al. [6,28] and Mercuri et al. [33].

As is apparent from the literature, the flow of tangential stresses in tapered beams is commonly determined on the basis of pure equilibrium considerations, assuming that the normal stresses follow Navier's formula and all displacements are so small that the equilibrium configuration coincides, for equilibrium purposes, with the initial configuration. The new shear formula proposed in this work is, as will be shown, more general, since it does not adopt any of these assumptions, which, incidentally, may not be satisfied in many applications.

3 THE BEAMLIKE SOLID MECHANICAL MODEL

The mechanical model used to derive the new shear formula proposed in section 4 is described in details in [8,34]. Here we briefly recall the model's main features, limiting the information to that needed to derive the new shear formula.

The beam is considered as a 3D body made of a collection of plane figures (corresponding to the transverse cross-sections) attached at a 3D curve (the beam centre-line, or axis). Each cross-section follows the beam axis, which may undergo large displacements. Moreover, in each cross-section an additional small displacement field is added, both in and out of plane, referred to here as 3D warping displacement (as specified below). Figure 1 shows a schematic of the beam reference and current states.

Two local triads of orthogonal unit vectors are introduced in Figure 1: $b_i=b_i(s)$ depends on the reference arc-length s, with b_1 tangential to the reference centre-line; $a_i=a_i(s,t)$ is the image of b_i in the current state and depends on s and the evolution parameter t. A third triad, c_i, pertains to a fixed Cartesian frame with origin chosen at will. The ranges of Greek and Latin indices are {2,3} and {1,2,3}, respectively; henceforth, the summation convention holds and the dependence on s and t is understood, hence omitted as long as no confusion arises.

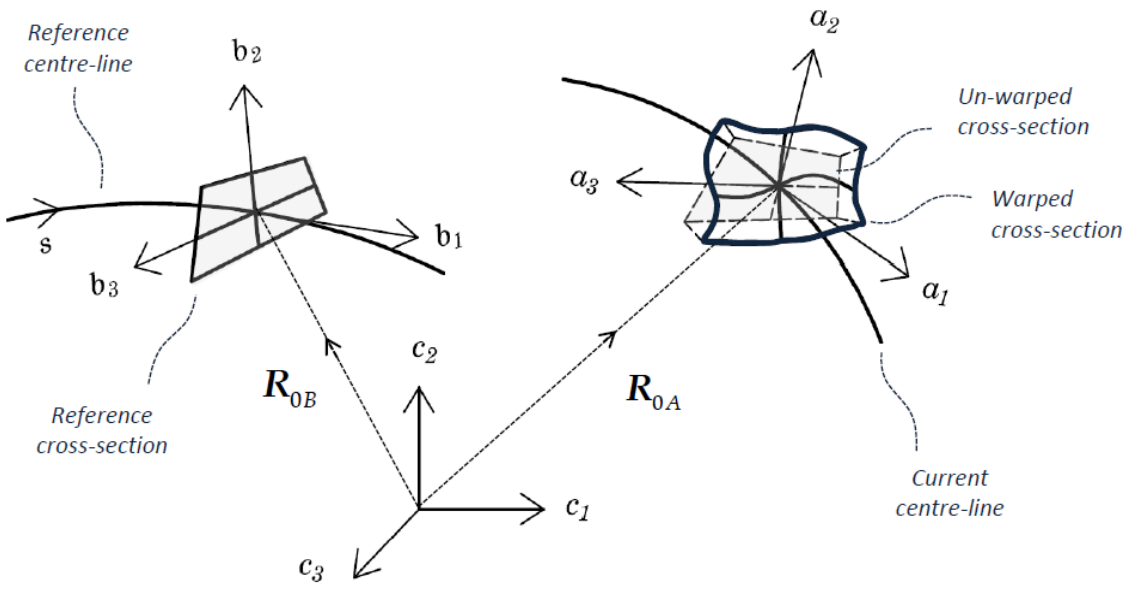

Figure 1: Reference (left) and current (right) states in terms of axes, cross-sections, local and global triads

The position of the beam points in the reference and current states are given by two mapping functions, R_B and R_A. The reference mapping function, R_B, is

$$R_B(z_i) = R_{0B}(z_1) + x_\alpha(z_i) b_\alpha(z_1) \tag{1}$$

where R_{0B} identifies the position of the reference axis, x_α denotes the coordinates of the cross-section points relative to such axis, and z_i are three time-independent mathematical variables, such that $z_1=s$ and z_α span a two-dimensional domain representing the prototype transverse cross-section. Specifically, for the tapered beams addressed in this work, we consider $x_i=\Lambda_{ij}z_j$, with $\Lambda_{11}=1$, $\Lambda_{22}=\Lambda_2(z_1)$, $\Lambda_{33}=\Lambda_3(z_1)$, and the other coefficients $\Lambda_{ij}=0$ identically.

The current mapping function is instead given by

$$R_A(z_i,t)=R_{0A}(z_1,t)+x_\alpha(z_i)a_\alpha(z_1,t)+w_k(z_i,t)a_k(z_1,t) \tag{2}$$

where w_k are the 3D warping displacement components relative to the local triad a_k.

Now we introduce the vector and tensor fields that describe the state of deformation of our body. The change in the beam's curvature between current and reference states, k, and that of the centre-line tangent between current and reference states, γ, are defined as follows:

$$\begin{aligned} k &= T^T k_A - k_B \\ \gamma &= T^T R'_{0A} - R'_{0B} \end{aligned} \tag{3}$$

where tensor $T=a_i\otimes b_i$, $\otimes$ is the usual tensor (or dyadic) product, prime denotes the derivative with respect to *s*, and vectors k_A and k_B describe the beam's curvatures in the current and reference states, respectively (details are in [34]). Vectors γ and k are referred to here as 1D strain measures. The 3D strain measure considered here is the Green-Lagrange strain tensor E, which is written in a form based on the assumptions of small strain and warping fields considered in this work (as in [8,34]). Specifically, we consider that the reference dimension of the cross-section, *h*, is much smaller than the reference length, *L*, of the centre-line; the beam's curvatures are much smaller than *1/h*; the warping fields, w_k, are small in the sense that their maximum order of magnitude is $h\varepsilon$, while the order of their derivative with respect to z_1 is at most $\varepsilon h/L$ ($\varepsilon<<1$ is a non-dimensional parameter). In general, all strain components are small in the sense their order of magnitude is at most ε. The strain tensor E is then expressed as

$$E\simeq\frac{T^TH+H^TT}{2}-I \tag{4}$$

where H is the gradient of transformation between the reference and current states, i.e. the derivative of the current map R_A with respect to the reference one R_B (as in [8,34]).

The stress is determined by assuming that the material composing the present beam behaves according to a linear elastic isotropic homogeneous constitutive relation; specifically,

we assume that the second (symmetric) Piola-Kirchhoff stress tensor, *S*, depends on the Green-Lagrange strain tensor, *E*, as follows:

$$S = 2\mu\, E + \lambda tr E\, I \tag{5}$$

where μ and λ are two known material parameters and *I* is the identity tensor [35].

The stress resultants over the cross-section reference domain Σ are expressed in terms of the first Piola-Kirchhoff stress tensor *P* as:

$$\begin{aligned} F &= \int_{\Sigma} P_{i1} a_i \\ M &= \int_{\Sigma} x_\alpha P_{i1}\, a_\alpha \wedge a_i \end{aligned} \tag{6}$$

where *F* and *M* are the force and moment resultants, respectively.

By applying the principle of the expended power to this 3D hyper-elastic beamlike body, the balance equations are obtained as in [8,34]. For example, equations for determining the warping fields w_k, in the case of vanishing volume and surface actions on the beam's lateral surface, can be derived via the following variational condition:

$$\delta \int_V \Phi = 0 \tag{7}$$

where $\Phi = S \cdot E/2$ and the symbol δ denotes the variation of the integral with respect to the warping fields w_k. Note that warping fields satisfying (7) can be obtained via the corresponding Euler-Lagrange equations [37,38]. In the general case, numerical methods are needed, but in some cases closed-form solutions can be found (see, e.g., [8,34]).

Omitting the details (available in [8,34]), and limiting to the case of non-prismatic beams with bi-tapered cross-sections (other effects, e.g. pre-twist, axial curvature, and material non-homogeneity, will be addressed in subsequent works), we now report the expressions for the strain fields E_{11}, E_{21}, and E_3, which describe the out-of-plane distortion of the cross-sections and will be necessary in section 4. They are expressed in the form:

$$\begin{aligned} E_{11} &= k_2 x_3 - k_3 x_2 + \gamma_1 + e_{1,1} \\ 2E_{21} &= e_{1,2} - k_1 x_3 + 2(1+\nu)(k_2 x_3 - k_3 x_2 + \gamma_1)\Lambda_2^{-1}\Lambda_2' x_2 + e_2 \\ 2E_{31} &= e_{1,3} + k_1 x_2 + 2(1+\nu)(k_2 x_3 - k_3 x_2 + \gamma_1)\Lambda_3^{-1}\Lambda_3' x_3 + e_3 \end{aligned} \tag{8}$$

where $E_{ij} = E \cdot b_i \otimes b_j$, υ is Poisson's ratio, commas indicate derivation with respect to x_i, and the scalar fields e_1, e_2, e_3, are solutions to the PDEs problem:

$$
\begin{aligned}
&e_{1,22} + e_{1,33} = 0 \quad in\ \Sigma \\
&e_{2,2} + e_{3,3} = f \quad in\ \Sigma \\
&e_{3,2} - e_{2,3} = g \quad in\ \Sigma \\
&(e_{1,2} - k_1 x_3) n_2 + (e_{1,3} + k_1 x_2) n_3 = 0 \quad on\ \partial\Sigma \\
&e_2 n_2 + e_3 n_3 = 0 \quad on\ \partial\Sigma
\end{aligned}
\tag{9}
$$

In (9), n_α are the components of the outward unit normal on $\partial\Sigma$, while functions f and g are defined as follows:

$$
\begin{aligned}
f &= 2(1+\nu)\left[x_2 k_3' + x_2 \left(\frac{\Lambda_3'}{\Lambda_3} + \frac{2\Lambda_2'}{\Lambda_2} \right) k_3 - x_3 k_2' - x_3 \left(\frac{\Lambda_2'}{\Lambda_2} + \frac{2\Lambda_3'}{\Lambda_3} \right) k_2 \right] \\
g &= -2\left[\nu x_2 k_2' + (1+\nu) x_2 \frac{\Lambda_2'}{\Lambda_2} k_2 + \nu x_3 k_3' + (1+\nu) x_3 \frac{\Lambda_3'}{\Lambda_3} k_3 \right]
\end{aligned}
\tag{10}
$$

For completeness, we also report the expressions for the components of the force and moment resultants, F_i and M_i, in the current local triad a_i:

$$
\begin{aligned}
F_1 &= YA\gamma_1 + Y\Gamma_1 k_1 + YX_1 k_1' \\
F_2 &= -YJ_3 k_3' + YJ_{23} k_2' - YJ_3' k_3 + YJ_{23}' k_2 \\
F_3 &= YJ_2 k_2' - YJ_{23} k_3' + YJ_2' k_2 - YJ_{23}' k_3 \\
M_1 &= GJ_1 k_1 + YV_1 \gamma_1 + YV_2 k_2 - YV_3 k_3 + YH_2 k_2' - YH_3 k_3' \\
M_2 &= YJ_2 k_2 - YJ_{23} k_3 + Y\Gamma_2 k_1 + YX_2 k_1' \\
M_3 &= YJ_3 k_3 - YJ_{23} k_2 - Y\Gamma_3 k_1 - YX_3 k_1'
\end{aligned}
\tag{11}
$$

where Y and G are the Young and shear moduli of the material, while the coefficients multiplying the 1D strain measures and their s-derivatives can be expressed as follows:

$$A = \int_\Sigma 1 \tag{12}$$

$$J_0 = \int_\Sigma x_2^2 + x_3^2 \tag{13}$$

$$J_1 = \int_\Sigma (e_{1,3}^{k_1} + x_2)^2 + (e_{1,2}^{k_1} - x_3)^2 \tag{14}$$

$$J_2 = \int_\Sigma x_3^2 \tag{15}$$

$$J_3 = \int_\Sigma x_2^2 \tag{16}$$

$$J_{23} = \int_\Sigma x_2 x_3 \tag{17}$$

$$X_1 = \int_\Sigma e_1^{k_1} \tag{18}$$

$$\Gamma_1 = \int_\Sigma e_{1,1}^{k_1} \tag{19}$$

$$X_2 = \int_\Sigma x_3 e_1^{k_1} \tag{20}$$

$$\Gamma_2 = \int_\Sigma x_3 e_{1,1}^{k_1} \tag{21}$$

$$X_3 = \int_\Sigma x_2 e_1^{k_1} \tag{22}$$

$$\Gamma_3 = \int_\Sigma x_2 e_{1,1}^{k_1} \tag{23}$$

$$V_1 = \rho'\rho^{-1} \int_\Sigma x_2 x_3 \tag{24}$$

$$V_2 = \rho'\rho^{-1} \int_\Sigma x_2 x_3^2 + \int_\Sigma x_2 e_3^{k_2} - x_3 e_2^{k_2} \tag{25}$$

$$V_3 = \rho'\rho^{-1} \int_\Sigma x_3 x_2^2 + \int_\Sigma x_3 e_2^{k_3} - x_2 e_3^{k_3} \tag{26}$$

$$H_2 = \int_\Sigma x_2 e_3^{k_2'} - x_3 e_2^{k_2'} \tag{27}$$

$$H_3 = \int_\Sigma x_3 e_2^{k_3'} - x_2 e_3^{k_3'} \tag{28}$$

The geometric parameters A, J_0, J_1, J_α, J_{23} are the beam's cross-sectional area, polar moment of inertia, Saint-Venant's torsion inertia, second moments of inertia, and mixed moment of inertia, respectively. The other coefficients (18)-(28), multiplying the 1D strain measures and their s-derivatives, depend solely on the geometric characteristics of the body through the shape of the cross-sectional domain Σ and the taper coefficients Λ_α. In particular, $\rho = \Lambda_3/\Lambda_2$, while quantities $e_j^{k_i}$ and $e_j^{k_i'}$ are the values obtained by solving the PDEs (9)-(10) for e_j when one superscript (e.g. k_2) is unitary and all others vanish. As an example, $e_2^{k_2}$ is the solution to the PDEs (9)-(10) when k_2=1, k_2'=0, k_3=0, k_3'=0. Details can be found in [8].

4 SHEAR FORMULA FOR BI-TAPERED BEAMS

In the previous section it has been shown that the scalar fields e_k are needed to determine the strain and stress fields. Equations (9)-(10) can generally be solved numerically, while an analytical solution can be found in only a few cases. However, apart from the direct determina-

tion of e_k, we can obtain analytical, closed-form expressions for the shear flow through the chords of the transverse cross-sections (e.g., AB in Figure 2) of our beamlike body. This in turn provides the mean shear stress over such chords, which is interesting from an engineering standpoint, as it can represent a good estimate of the shear stress at the points of the chords if their length is small enough.

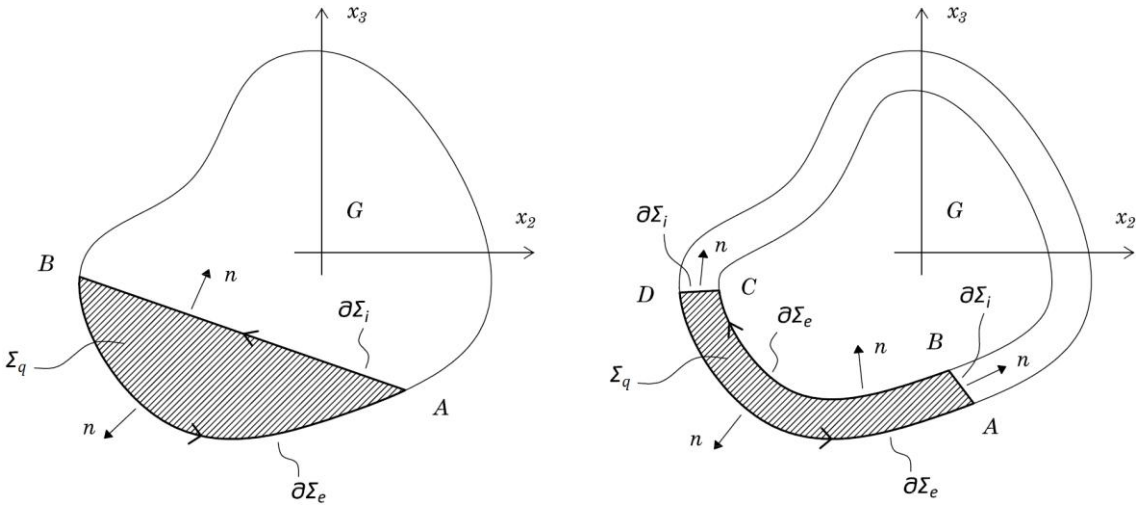

Figure 2: Transverse cross-sections, solid (left) and hollow (right)

With this aim, we introduce some notation. Figure 2 shows a solid (left) and a hollow (right) cross-section, split in two: the dashed sub-domain is called Σ_q; its boundary (moving counter-clockwise) consists of internal lines $\partial\Sigma_i$ (contained in the cross-section) and external lines $\partial\Sigma_e$. The total shear flow q through the entire set of internal lines is

$$q = \int_{\partial\Sigma_i} C_{1\alpha} n_\alpha \tag{29}$$

In the case of the hollow cross-section in Figure 2 (right), for instance, equation (29) provides the sum of the shear flows through AB and CD. The partition of the domain and its boundaries, plus the definition of the shear flow (29), also apply to multi-connected cross-sections, although they are not shown in Figure 2. Equation (29), plus (8)-(10) and standard integration techniques based on Green's formulas, yield

$$q = -YS_2k_2' + YS_3k_3' - YZ_2k_2 + YZ_3k_3 + YZ_1\gamma_1 \tag{30}$$

where the coefficients S_α and Z_i are given by the following surface and line integrals

$$
\begin{aligned}
S_2 &= \int_{\Sigma_q} x_3 \\
S_3 &= \int_{\Sigma_q} x_2 \\
Z_2 &= \int_{\partial\Sigma_e} x_3(\Lambda_2^{-1}\Lambda_2' x_2 n_2 + \Lambda_3^{-1}\Lambda_3' x_3 n_3) \\
Z_3 &= \int_{\partial\Sigma_e} x_2(\Lambda_2^{-1}\Lambda_2' x_2 n_2 + \Lambda_3^{-1}\Lambda_3' x_3 n_3) \\
Z_1 &= \int_{\partial\Sigma_i} \Lambda_2^{-1}\Lambda_2' x_2 n_2 + \Lambda_3^{-1}\Lambda_3' x_3 n_3
\end{aligned}
\tag{31}
$$

Equation (30) is the new closed-form formula for the shear flow in bi-tapered beams susceptible to large deflections, which extends Jourawski's formula (valid only for prismatic beams in a linear setting). The first two terms in (30) account for the spanwise variation of the bending curvatures (i.e., their *s*-derivative) via their product with the first moments of area of the dashed domain. The third and fourth addends are directly proportional to the bending curvatures, and explicitly account for the taper via a kind of second moments of inertia of the cross-section boundary; the last term depends on the axial elongation γ_1 via a kind of first moment of inertia of the cross-section boundary. Note also that the latter three addends, proportional to Z_i, vanish identically if the beam is not tapered (in fact, for prismatic beams Λ'_α=0). Moreover, for prismatic beams in a linear setting the shear formula (30) reduces exactly to Jourawski's, as the *s*-derivative of the bending curvatures turn out to be directly proportional to the shear forces in the beam reference state.

To compare the results of (30) with those of other shear formulas, it is convenient to focus on flexure and traction without torsion and express the shear flow in terms of stress resultants rather than 1D strains. By combining (11) and (30) for flexure and traction and assuming that x_2, x_3 are central and principal axes of inertia for the cross-sectional domain, (30) becomes

$$
q = -\frac{F_3 S_2}{J_2} - \frac{F_2 S_3}{J_3} + \frac{F_1 Z_1}{A} - \frac{M_2 \Pi_2}{J_2} + \frac{M_3 \Pi_3}{J_3} \tag{32}
$$

In (32), Π_α are geometric functions of Z_α, S_α and Λ_α, as follows

$$
\begin{aligned}
\Pi_2 &= Z_2 - S_2(\Lambda_2^{-1}\Lambda_2' + 3\Lambda_3^{-1}\Lambda_3') \\
\Pi_3 &= Z_3 - S_3(\Lambda_3^{-1}\Lambda_3' + 3\Lambda_2^{-1}\Lambda_2')
\end{aligned}
\tag{33}
$$

F_1, F_α, M_α are the components of the force and moment resultants with respect to the *current* local triad a_i, and A and J_α are the cross-sectional area and second moments of inertia.

Note that the first two terms in (32) are similar to those of the linear theory of prismatic beams; however, the transverse forces F_α are along the *current* unit vectors a_α (not the *reference* ones), and J_α depend on s. The last three terms of (32) are proportional to the *current* bending moments M_α and axial force F_1, which are absent in the linear theory of prismatic beams and explicitly depend on the taper coefficients Λ_α and their s-derivative. However, if the current and reference states of the beam are indistinguishable (i.e., in a linear setting) and the beam is prismatic (i.e., $\Lambda_\alpha'=0$), Jourawski's formula is clearly re-obtained.

We now show how the shear formula (30), (32) can furnish results of engineering interest.

4.1 Bi-tapered rectangular cross-sections

Consider a beam with rectangular cross-sections of width $2h_2$ and height $2h_3$, bi-tapered from the root to the tip as shown in Figure 3, and loaded by a flap-wise dead force F at the tip.

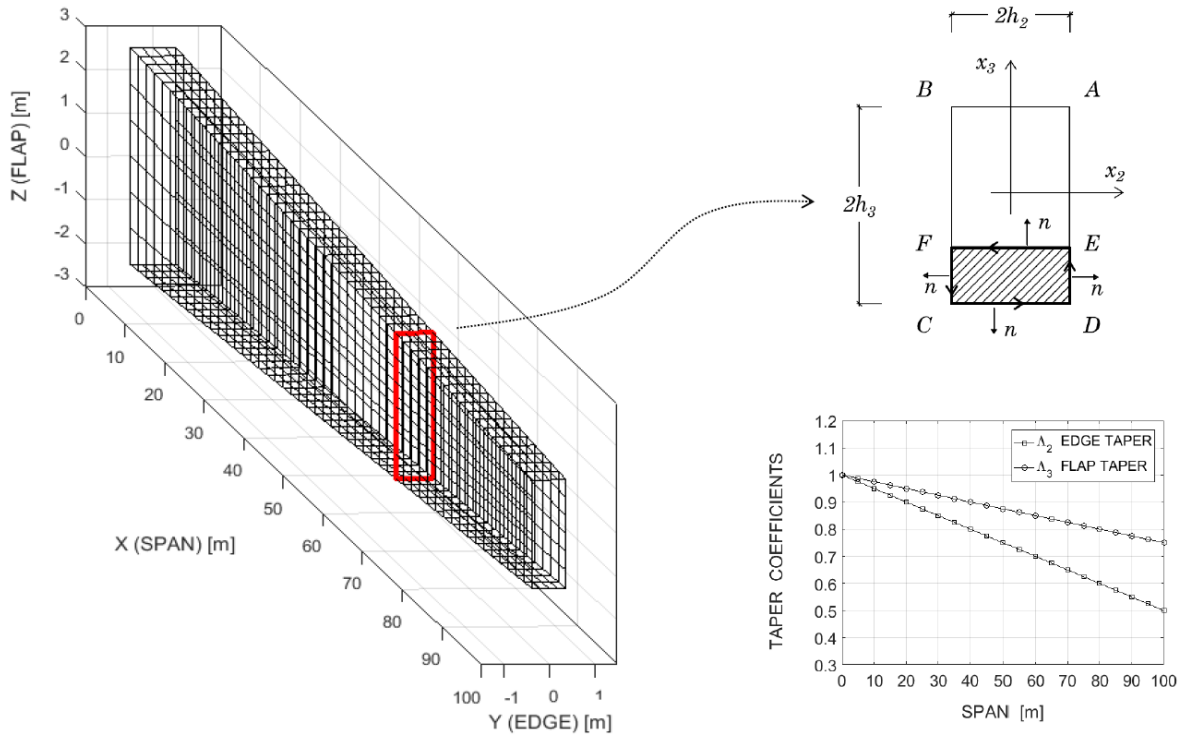

Figure 3: Beam with linearly bi-tapered rectangular cross-sections (left) and its taper coefficients (right)

The considered loading condition induces a deflection such that $k_3=0$; then, in this case, the shear formula (30) yields

$$q = -ES_2k_2' - EZ_2k_2 + EZ_1\gamma_1 \tag{34}$$

Moreover, for the present geometry, the coefficients S_2, Z_2, Z_1 are given by the relations

$$
\begin{aligned}
S_2 &= h_2(x_3^2 - h_3^2) \\
Z_2 &= h_2(x_3^2 - h_3^2)\Lambda_2^{-1}\Lambda_2' - 2h_2h_3^2\Lambda_3^{-1}\Lambda_3' \\
Z_1 &= 2h_2x_3\Lambda_3^{-1}\Lambda_3'
\end{aligned}
\tag{35}
$$

which, in turn, enable writing equation (34) in the form

$$
\frac{q}{2h_2} = -\left(Ek_2' + Ek_2\Lambda_2^{-1}\Lambda_2'\right)\frac{x_3^2 - h_3^2}{2} + Ek_2\Lambda_3^{-1}\Lambda_3'h_3^2 + E\gamma_1\Lambda_3^{-1}\Lambda_3'x_3 \tag{36}
$$

Equation (36) explicitly shows how $q/2h_2$, i.e., the mean shear stress over a chord parallel to the width of the cross-section, depends on the 1D strains and geometric characteristics (taper included) of the bi-tapered beam. We can also express (36) in terms of stress resultants, rather than 1D strains, to compare its results with those of other formulas. We obtain

$$
\frac{q}{2h_2} = -\frac{F_3 - 3M_2\Lambda_3^{-1}\Lambda_3'}{J_2}\frac{x_3^2 - h_3^2}{2} + \frac{F_1}{A}\Lambda_3^{-1}\Lambda_3'x_3 + \frac{M_2}{J_2}\Lambda_3^{-1}\Lambda_3'h_3^2 \tag{37}
$$

where F_1, F_3, M_2 are axial and transverse forces and bending moment along the *current* local triad a_i; A, J_2 are the cross-sectional area and second moment of inertia with respect to x_2.

We also report (37) in terms of stress resultants with respect to the *reference* local triad b_i, which is consistent with the Cartesian frame X,Y,Z in Figure 3. To this end, if θ is the angle of rotation of the current local triad a_i with respect to the reference one about $b_2 \equiv Y$, we obtain

$$
\frac{q}{2h_2} = \eta_T F_Z + \eta_N F_X + \eta_M M_Y \tag{38}
$$

where F_X, F_Z, M_Y are respectively the axial and transverse forces and bending moment along the *reference* triad b_i. The geometric quantities η_T, η_N, η_M weight the contribution of the *reference* stress resultants to the mean shear stress $q/2h_2$ and are given by

$$
\begin{aligned}
\eta_T &= \frac{(h_3^2 - x_3^2)\cos\theta}{2J_2} - \frac{\Lambda_3^{-1}\Lambda_3'x_3\sin\theta}{A} \\
\eta_N &= \frac{\Lambda_3^{-1}\Lambda_3'x_3\cos\theta}{A} + \frac{(h_3^2 - x_3^2)\sin\theta}{2J_2} \\
\eta_M &= \frac{\Lambda_3^{-1}\Lambda_3'(3x_3^2 - h_3^2)}{2J_2}
\end{aligned}
\tag{39}
$$

It is now evident how (37) extends Jourawski's formula. The mean shear stress over a chord parallel to the width of the cross-section (Figure 3) consists of a first term proportional to the transverse force F_3, similar to that of the linear theory of prismatic beams [5]. We recall

that F_3 is the shearing force along the *current* unit vector a_3, and that large displacements and rotations may separate the current beam state and local triad from the reference ones; moreover, the moment of inertia J_2 depends on s. The right side of (37) contains terms proportional to the *current* bending moment M_2 and axial force F_1, which are absent in the linear theory of prismatic beams and explicitly depend on the taper coefficient Λ_3 and its s-derivative. If the current and reference states of the beam are adjacent (i.e., for small displacements and rotations), the shear flow (37) coincides with that given by Bleich [10], Cortinez [15] and Taglialegne [16], among others (see appendix). Furthermore, if the beam is prismatic (i.e., A and J_2 do not depend on s, and the s-derivatives of the taper coefficients vanish), we re-obtain the well-known Jourawski's solution [5].

4.2 Bi-tapered elliptical cross-sections

Consider a bi-tapered beam with elliptic cross-sections of major semi-axes h_2 (edgewise) and h_3 (flapwise), bi-tapered from root to tip according to the taper coefficients in Figure 4.

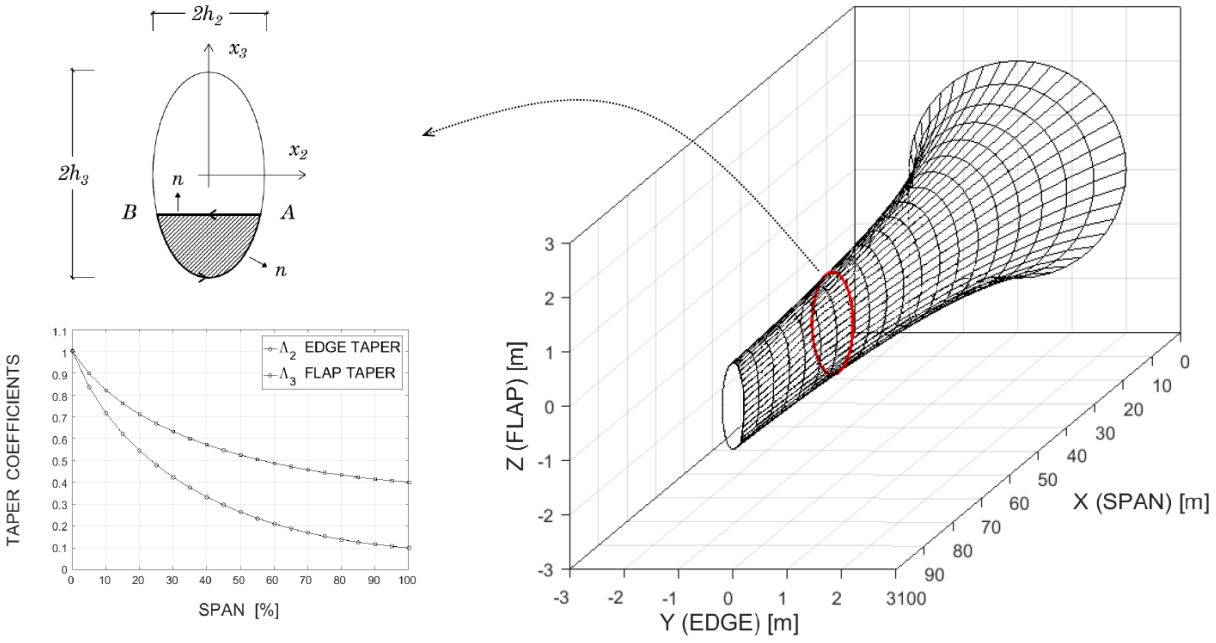

Figure 4: Beam with bi-tapered elliptical cross-sections (left) and its taper coefficients (right)

Let the beam be loaded by a flapwise dead force F at the tip, which induces a deflection such that k_3=0; then, the shear formula (30) takes the form

$$q = -ES_2k_2' - EZ_2k_2 + EZ_1\gamma_1 \tag{40}$$

where the coefficients S_2, Z_2, Z_1 are now given by

$$
\begin{aligned}
S_2 &= 2d_2(x_3^2 - h_3^2)/3 \\
Z_2 &= 2d_2\Lambda_3^{-1}\Lambda_3'(x_3^2 + 2h_3^2)/3 - 2d_2\Lambda_2^{-1}\Lambda_2'(x_3^2 - h_3^2)/3 \\
Z_1 &= 2d_2\Lambda_3^{-1}\Lambda_3' x_3
\end{aligned}
\tag{41}
$$

and $2d_2$ is the length of AB (parallel to x_2) in Figure 4. By combining (40)-(41), we get

$$
\frac{q}{2d_2} = -\left(Ek_2' - Ek_2\rho'\rho^{-1}\right)\frac{x_3^2 - h_3^2}{3} + Ek_2\Lambda_3^{-1}\Lambda_3' h_3^2 + E\gamma_1\Lambda_3^{-1}\Lambda_3' x_3 \tag{42}
$$

which can also be expressed in terms of stress resultants as follows

$$
\frac{q}{2d_2} = -\frac{F_3 - 4M_2\Lambda_3^{-1}\Lambda_3'}{J_2}\frac{x_3^2 - h_3^2}{3} + \frac{F_1}{A}\Lambda_3^{-1}\Lambda_3' x_3 + \frac{M_2}{J_2}\Lambda_3^{-1}\Lambda_3' h_3^2 \tag{43}
$$

Recall that F_1, F_3, M_2 are components of the resultants along the *current* local triad a_i; A, J_2 are the cross-sectional area and second moment of inertia; and $\rho = \Lambda_3/\Lambda_2$. Also in this case we can express q in terms of stress resultants along the *reference* local triad b_i

$$
\frac{q}{2d_2} = \eta_T F_Z + \eta_N F_X + \eta_M M_Y \tag{44}
$$

where F_X, F_Z, M_Y are the axial and transverse forces and bending moment with respect to b_i, while the geometric coefficients η_T, η_N, η_M are now given by

$$
\begin{aligned}
\eta_T &= \frac{(h_3^2 - x_3^2)\cos\theta}{3J_2} - \frac{\Lambda_3^{-1}\Lambda_3' x_3 \sin\theta}{A} \\
\eta_N &= \frac{\Lambda_3^{-1}\Lambda_3' x_3 \cos\theta}{A} + \frac{(h_3^2 - x_3^2)\sin\theta}{3J_2} \\
\eta_M &= \frac{\Lambda_3^{-1}\Lambda_3'(4x_3^2 - h_3^2)}{3J_2}
\end{aligned}
\tag{45}
$$

Note that also in this case we can recognize the term proportional to F_3 as similar to that of the linear theory of prismatic beams (apart from the fact that it is parallel to the *current* unit vector a_3, and J_2 depends on s), along with the additional terms associated to the *current* bending moments M_2 and axial force F_1 (which are proportional to the taper coefficient Λ_3 and its s-derivative). Moreover, if the beam is prismatic and undergoes small displacements and rotations, our results reduce once again to those obtainable with Jourawski's formula.

Other examples will be presented in subsequent works. Here we now proceed to evaluate the effectiveness of the model and formulas presented so far by performing comparisons with the numerical results of nonlinear 3D-FEM analyses.

5 NUMERICAL EXAMPLES

In this section the results furnished by the model and formulas presented in the foregoing are compared with those from other formulas available in the literature and nonlinear 3D-FEM analysis, for two benchmark cases that correspond to the cases discussed analytically in sections 4.1 and 4.2. In particular, the model and formulas presented in sections 3 and 4 have been implemented in a numerical code in Matlab, henceforth referred to as 3D-BLM. The 3D-FEM analyses have been performed in Ansys using a fine mesh of solid tetrahedral elements with 10 nodes [39]. The results of the nonlinear 3D-FEM analyses are taken as reference values against which all the other results will be compared.

The two test cases mentioned above address bi-tapered beams that are fixed at the root and loaded at the tip by a transverse force. The two beams have different cross-sectional shapes and taper coefficients (see Figures 3 and 4, respectively). In both cases our results in terms of shear stresses are based on the shear formula (32) and on its specialized formulations for the rectangular (37) and elliptical (43) bi-tapered cross-sections. Such results are moreover compared to corresponding results available in the literature: the formulas of Jourawski [5] and Bleich [10], among others, have been considered in the first case; the analytical solutions of Migliaccio and Ruta [8,34] in the second case.

5.1 Test case 1

The beam with rectangular cross-section considered here is 100 m long. The section's dimensions are $2d_2 = 1$ m (edgewise) and $2d_3 = 5$ m (flapwise) at the root and reduce linearly from the root to the tip, as shown in Figure 3. Young's modulus is 70 GPa, and Poisson's ratio is 0.25. The beam is clamped at the root; the load at the tip is a flapwise dead force, F, inducing a deflection in the X-Z plane of Figure 3.

In general, 3D-BLM can provide several meaningful information about the mechanical response of a beam, including, for example, centre-line displacements, curvature changes, triad rotations, stress and strain fields, and stress resultants, as shown in previous works (e.g. [8,34,40,41]). In this paper the focus is on the shear formula introduced in section 4 and the agreement among its results with those of nonlinear 3D-FEM simulations.

Hereafter we summarize the predictions of 3D-BLM in terms of stress fields at four reference cross-sections, whose distance from the root is equal to respectively 5%, 35%, 65%, 95% of the overall beam length, and for two values of tip-force, namely F = 50 kN and F = 5000 kN. Figures 16 and 17 show the results obtained for the longitudinal normal stress

C_{XX}; Figures 18 and 19 report the results for the transverse shear stress C_{ZX}, where X and Z are directions parallel to the axis of the Cartesian reference frame in Figure 3.

Looking at the numerical results obtained, we note that the normal stresses follow a Navier-like distribution in the transverse cross-sections (i.e., they are almost linear in x_3), while the shear stress distributions are quite different from those predictable by the linear theory of prismatic beams, as the transverse shear stress at the cross-section boundary of non-prismatic beams does not generally vanish, and the maximum value may not occur at the point corresponding to the centroid of Σ. This is confirmed, in particular, by the results reported in Figure 18: blue lines are the results of our model (label 3D-BLM); red marks denote the results from nonlinear 3D-FEM; yellow lines are the results obtained by Jourawski's formula (linear theory of prismatic beams) for the present tapered beam as if it were a stepped beam (label J-STEP); finally, black lines correspond to the results obtained by exploiting Bleich's formula, which is still based on linear beam theory but accounts for the effects of taper as discussed in the introduction and in [10] (label B-ET-AL).

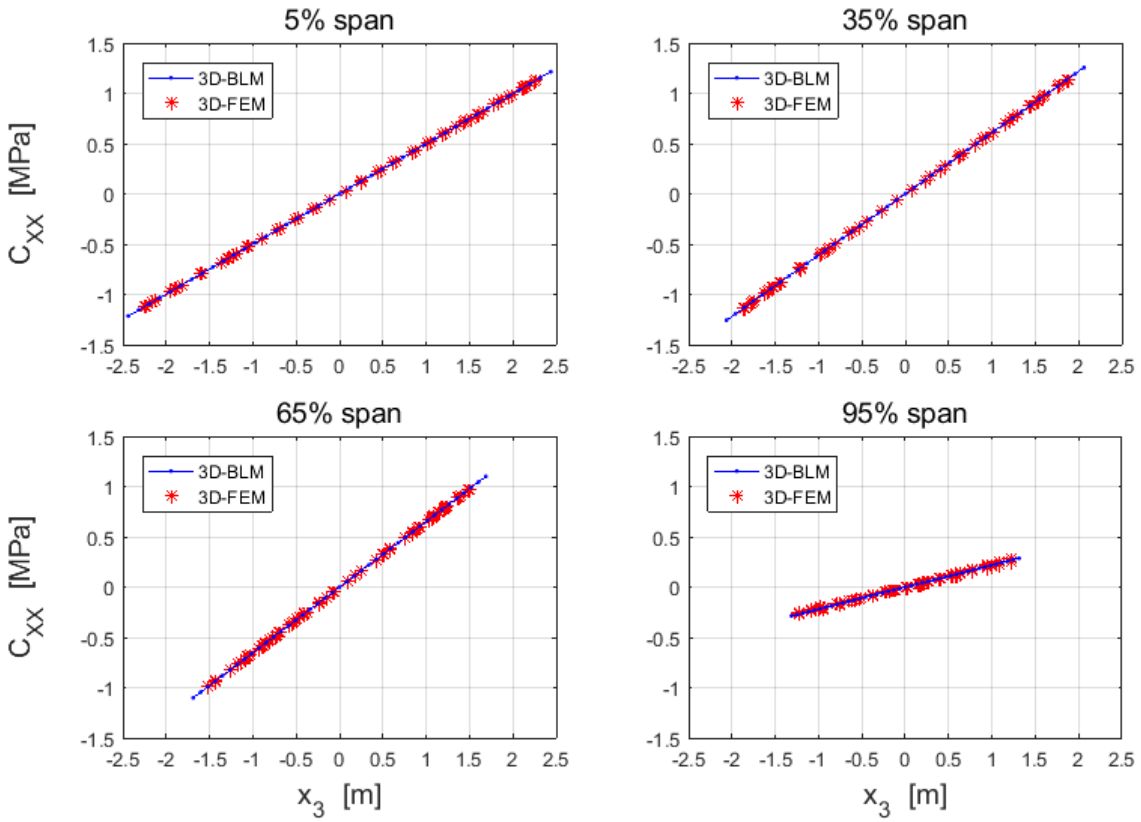

Figure 16: Longitudinal normal stress C_{XX} in the cross-sections at 5%, 35%, 65%, 95% span for F = 50 kN

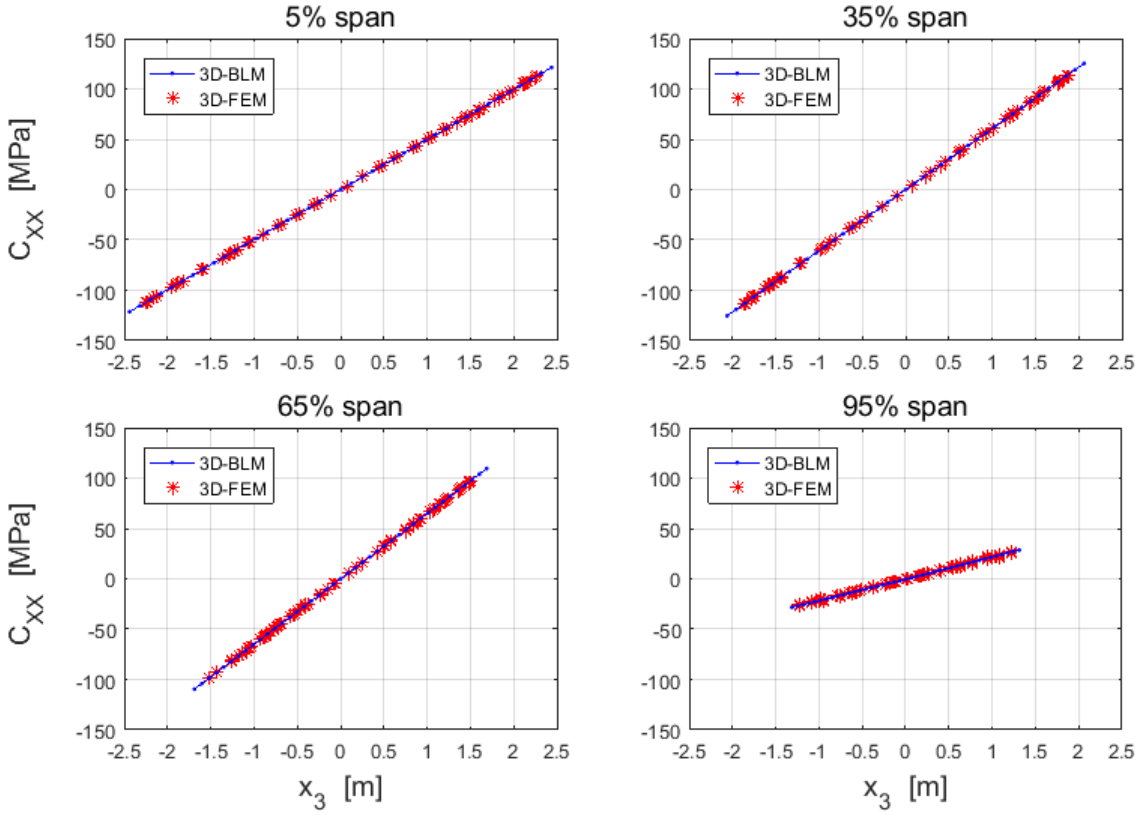

Figure 17: Longitudinal normal stress C_{XX} in the cross-sections at 5%, 35%, 65%, 95% span for F = 5000 kN

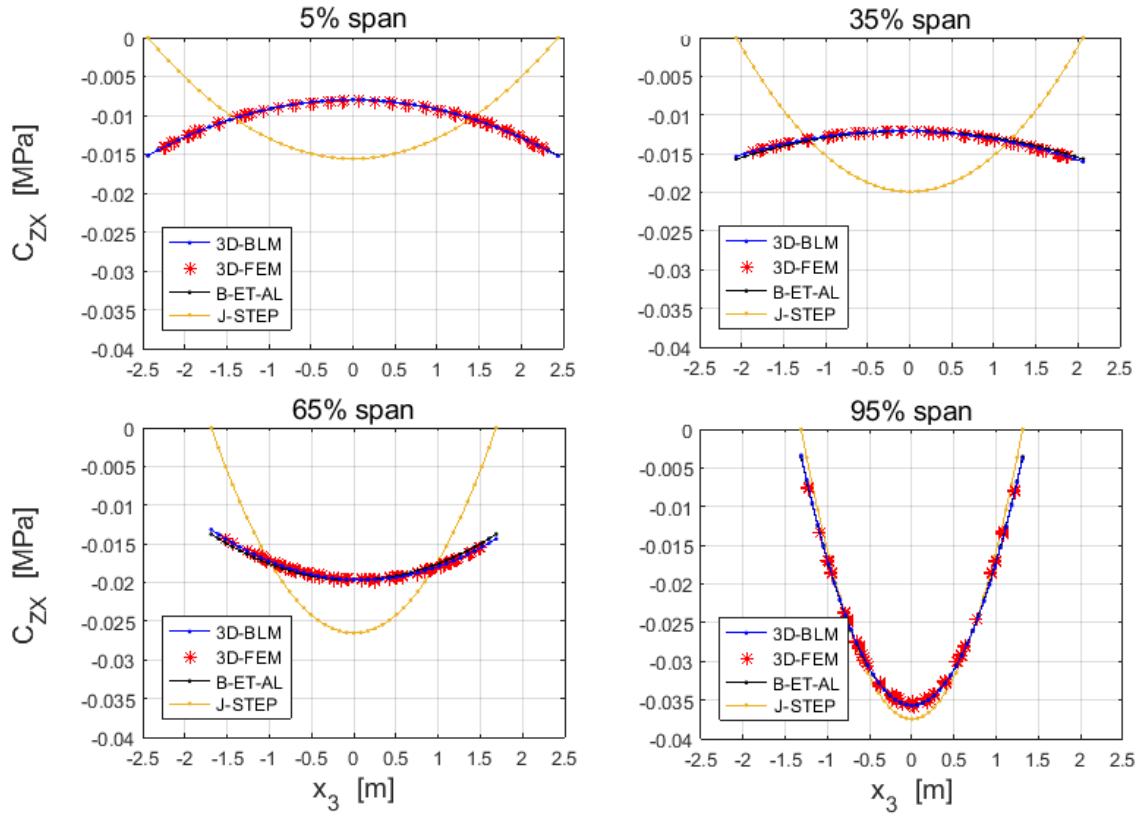

Figure 18: Transverse shear stress C_{ZX} in the cross-sections at 5%, 35%, 65%, 95% span for F = 50 kN

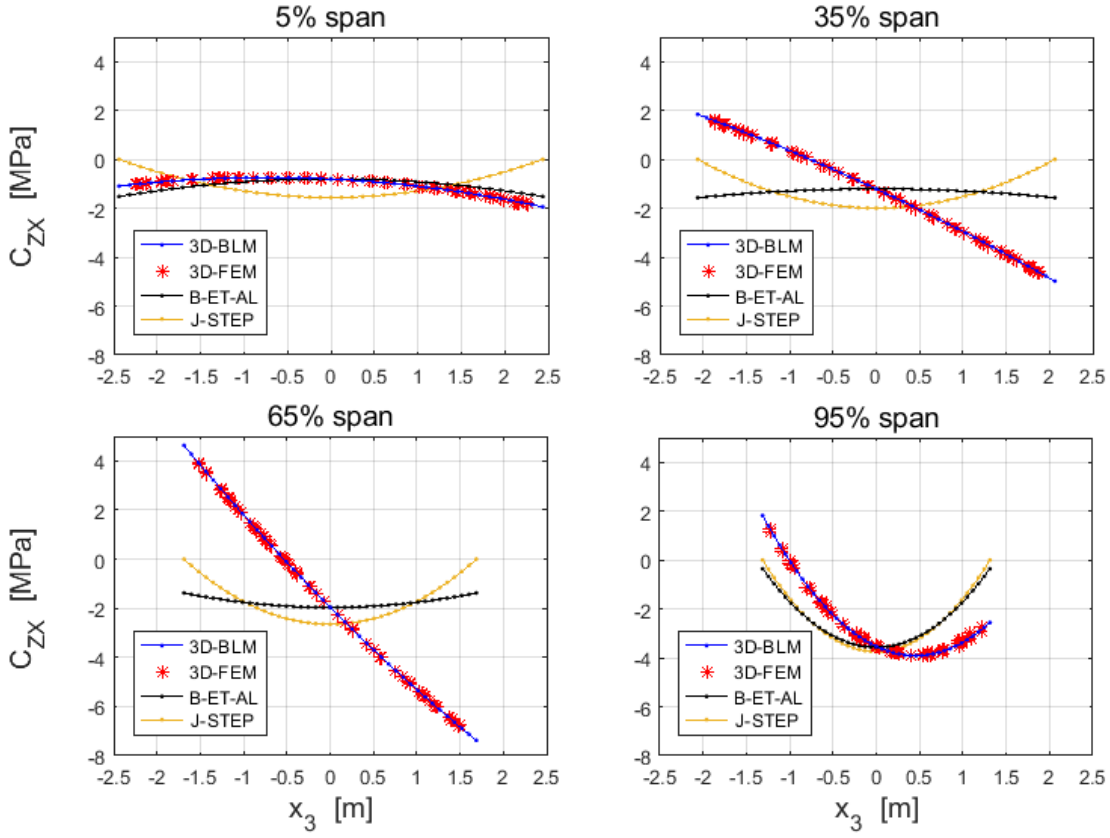

Figure 19: Transverse shear stress C_{ZX} in the cross-sections at 5%, 35%, 65%, 95% span for F = 5000kN

Figures 18 and 19 clearly show that modelling a tapered beam as a stepped beam and using Jourawski's solution for each segment of the stepped beam does not provide good results, except for a limited region close to the beam's tip where the effects of the taper related to the bending moment fall to zero (label J-STEP). In addition, Jourawski's formula does not allow satisfying the condition of non-vanishing transverse shear stress on the cross-section boundary. Bleich's solution does not suffer from such drawback and may provide good results for tapered beams undergoing small displacements and strains, provided the actual shape of the beam does not differ too much from the reference one. This is also confirmed by the plots in Figure 18, regarding the low-value tip-force (F=50kN): in such case the results of 3D-FEM, 3D-BLM and B-ET-AL almost coincide. When the tip-force increases (see, e.g., Figure 19), and the beam's actual and reference shapes become too distant, the only results very close to those of nonlinear 3D-FEM are those furnished by 3D-BLM.

5.2 Test case 2

The bi-tapered beam considered here is 100 m long. Its cross-sections are elliptically shaped and are tapered from the root to the tip of the beam, as shown in Figure 4. The lengths of the major semi-axis at the root are d_2 = 2.0 m (edgewise) and d_3 = 2.0 m (flapwise). Those of the other cross-sections vary according to the taper coefficients in Figure 4. The material Young's modulus is 70 GPa; the Poisson's ratio is 0.25. The beam is clamped at the root and a flapwise dead force, *F*, acts at the tip and induces a deflection in the X-Z plane in Figure 4.

Before going on to the comparison with the 3D-FEM results, we note that in this case the elliptical shape of the cross-section allows for analytically solving the PDEs problem (9)-(10). As the analytical closed-form solution to the problem is available in [8,34], it is worth checking the approximations of the shear stresses obtained by the shear formula (43) by comparing them with the analytical solution given in [8,34].

Figure 20 shows the results obtained for the shear stress C_{ZX}, at four cross-sections (at 5%, 35%, 65%, 95% span), for F = 50 kN. The curves drawn in blue, red, cyan, and magenta colours are the results yielded by the analytical solution of 3D-BLM [8,34], calculated for different values of x_2 (namely: $x_2 = 0$, $x_2 = 0.3h_2$, $x_2 = 0.6h_2$, $x_2 = 0.9h_2$); the green curve (labelled 3D-BLM-SF) corresponds to the results of 3D-BLM based on the shear formula presented in section 4.2. Note that the shear stress C_{ZX} obtained with the analytical solution depends pointwise on both x_3 and x_2 coordinates, while that assessed by the shear formula (43) only depends on x_3 and corresponds to the mean value of C_{ZX} along the chord x_3 = const. Some error is expected when using the shear formula; however, it is worth observing that such differences are limited to the first half of the beam, where the ratio between the major semi-axes h_3/h_2 goes to 1 at the circular root section. Toward the tip the ratio h_3/h_2 increases (up to 4 at the tip section), the dependence on x_2 becomes negligible, and all aforementioned four lines (blue, red, cyan, magenta) nearly coincide. Accordingly, and predictably, the more we move toward the tip section of the present beam, the closer will the mean shear stress given by the shear formula be to the actual shear stress over the considered chord.

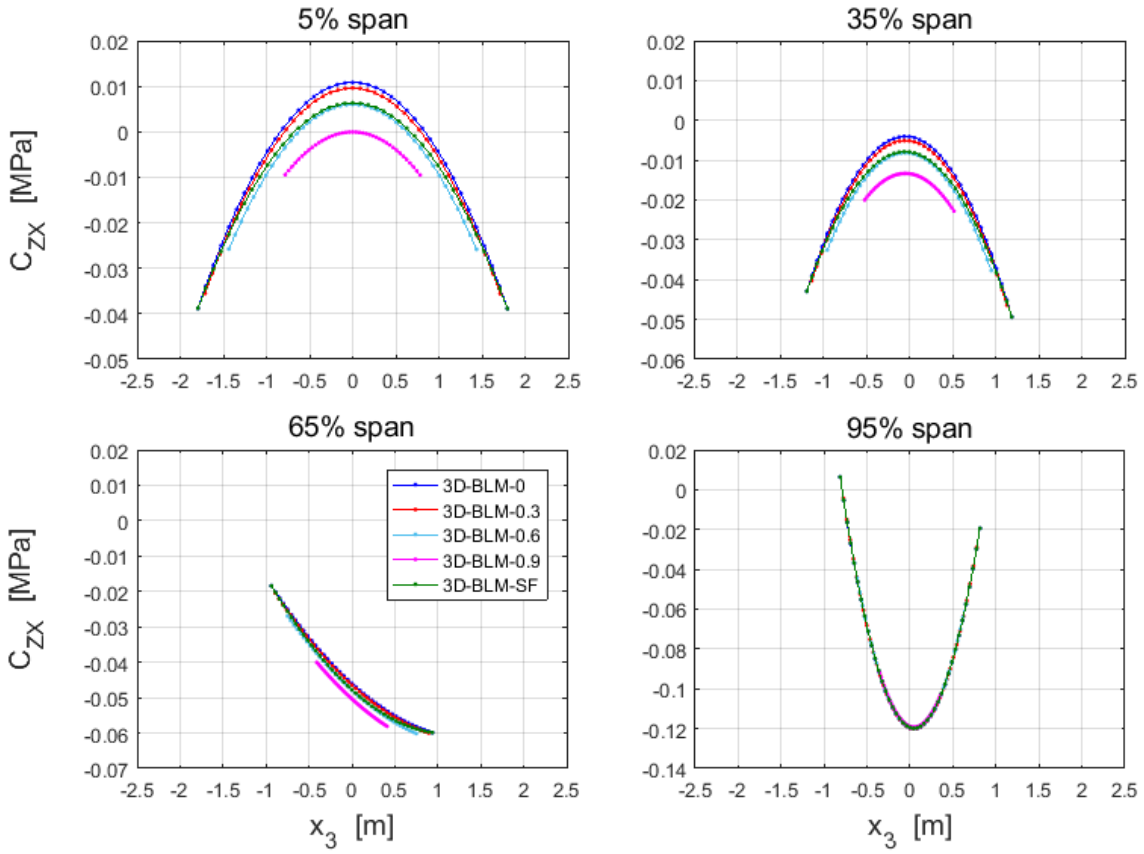

Figure 20: Analytical solution versus shear formula - C_{ZX} at 5%, 35%, 65%, 95% span for F = 50 kN

Now we continue with the comparisons by also including the results of 3D-FEM. In particular, we focus on the stresses along the vertical major-axis, x_3, of the cross-sectional domain. Figure 21 reports the shear stress C_{ZX} at the same four reference cross-sections as above (5 %, 35 %, 65 %, 95 % span), for F = 50 kN: blue lines are the results based on the analytical solution (label 3D-BLM-0); green lines correspond to the shear formula results (label 3D-BLM-SF); red marks denote the finite element results (label 3D-FEM-0). Note that the results of the analytical solution almost coincide with 3D-FEM, and that the shear formula also provides a good estimation of the shear stress (which is closer to the actual shear stress the more we move toward the tip section). Actually, results of this kind are to be expected, as the shear formula can only furnish the mean value of the shear stress along the considered chords.

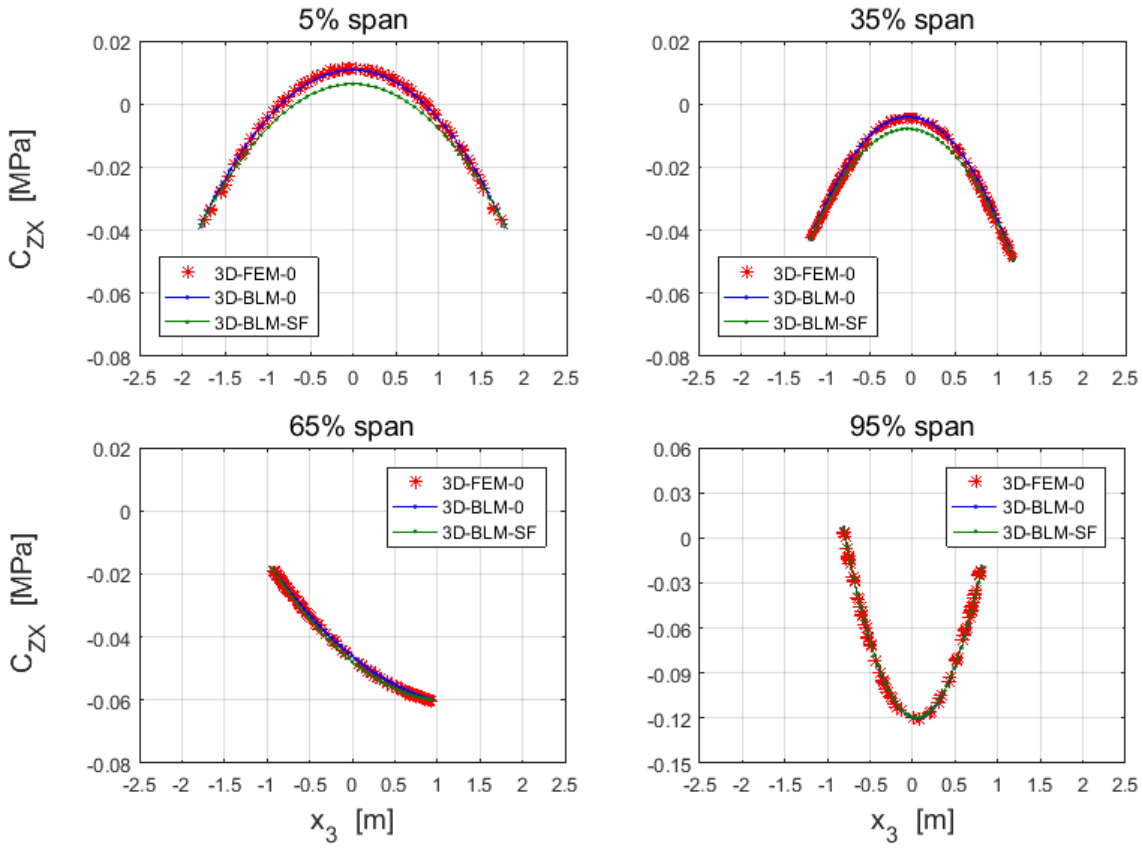

Figure 21: Transverse shear stress C_{ZX} in the cross-sections at 5%, 35%, 65%, 95% span for F = 50 kN

For completeness, we conclude by reporting the results obtained for the shear stress C_{ZX}, for a larger tip-force, F = 1000 kN (Figure 22), as well as those obtained for the normal stress C_{XX}, both for F = 50 kN and F = 1000 kN (Figures 23-24), which once again follow a Navier-like distribution along the cross-sectional domain, thus confirming the result already found in the first test case as well as in previous works, e.g. [8,34].

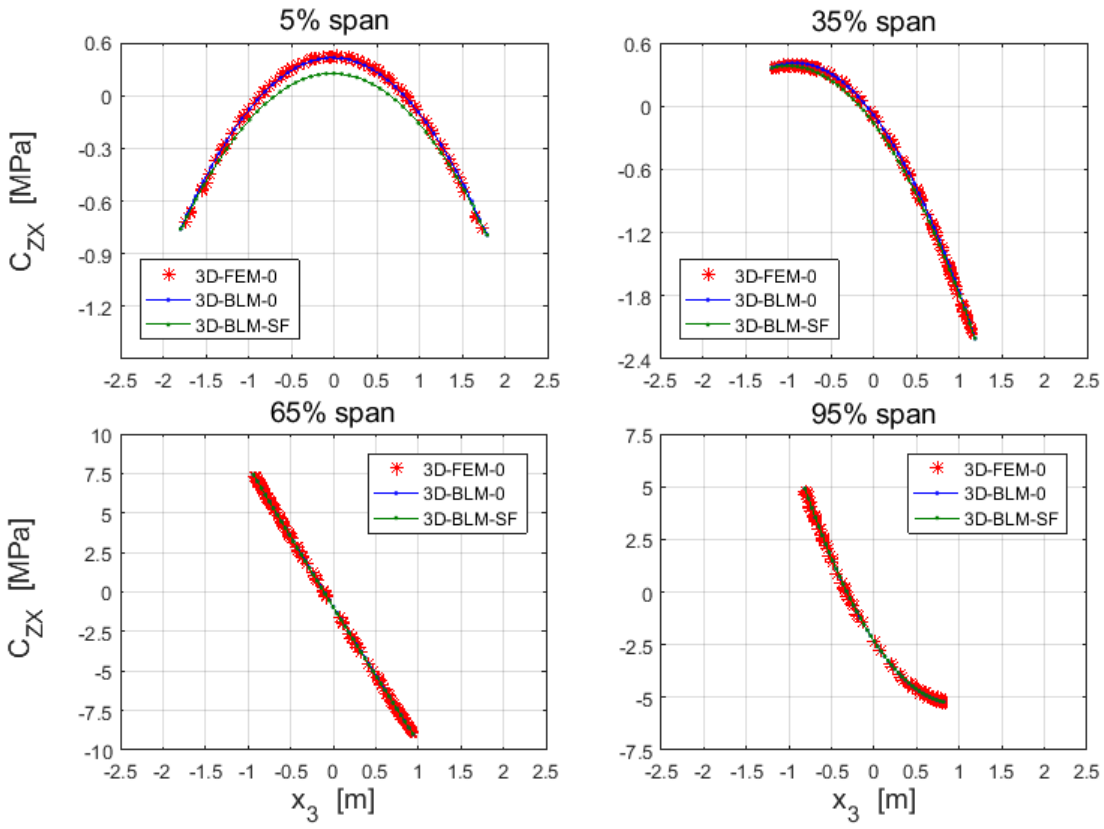

Figure 22: Transverse shear stress C_{ZX} in the cross-sections at 5%, 35%, 65%, 95% span for F = 1000 kN

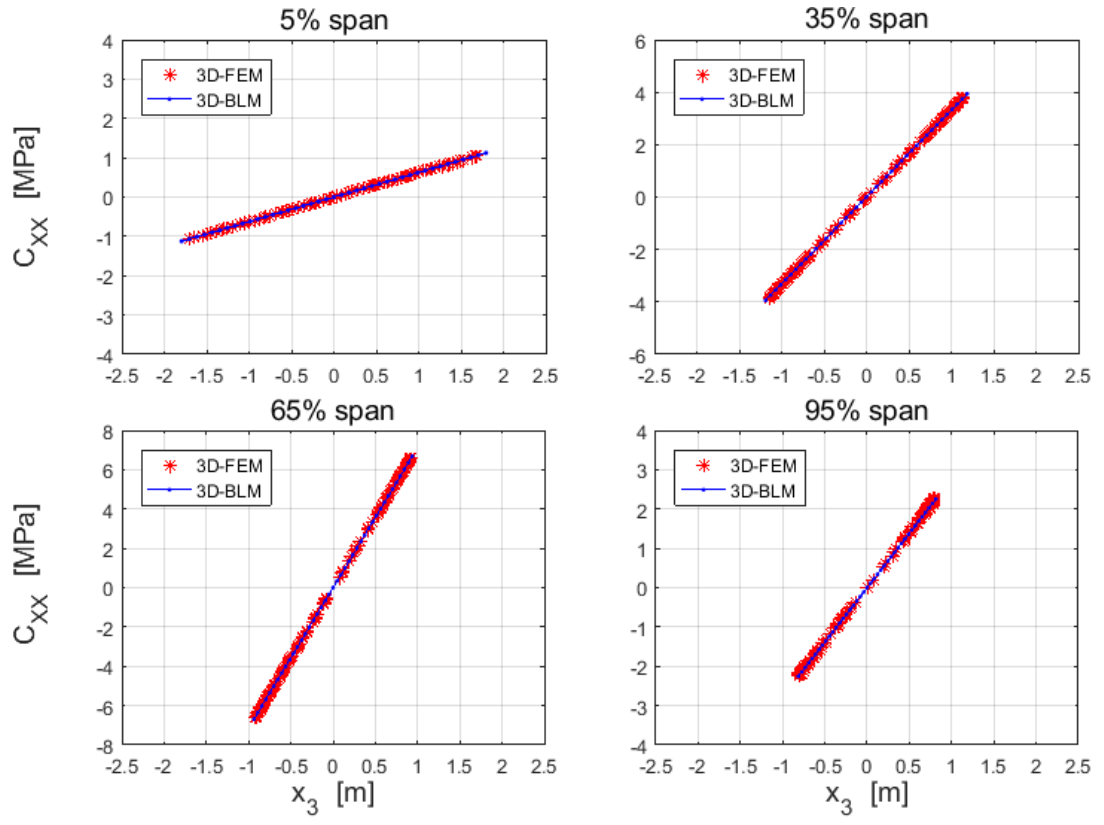

Figure 23: Longitudinal normal stress C_{XX} in the cross-sections at 5%, 35%, 65%, 95% span for F = 50 kN

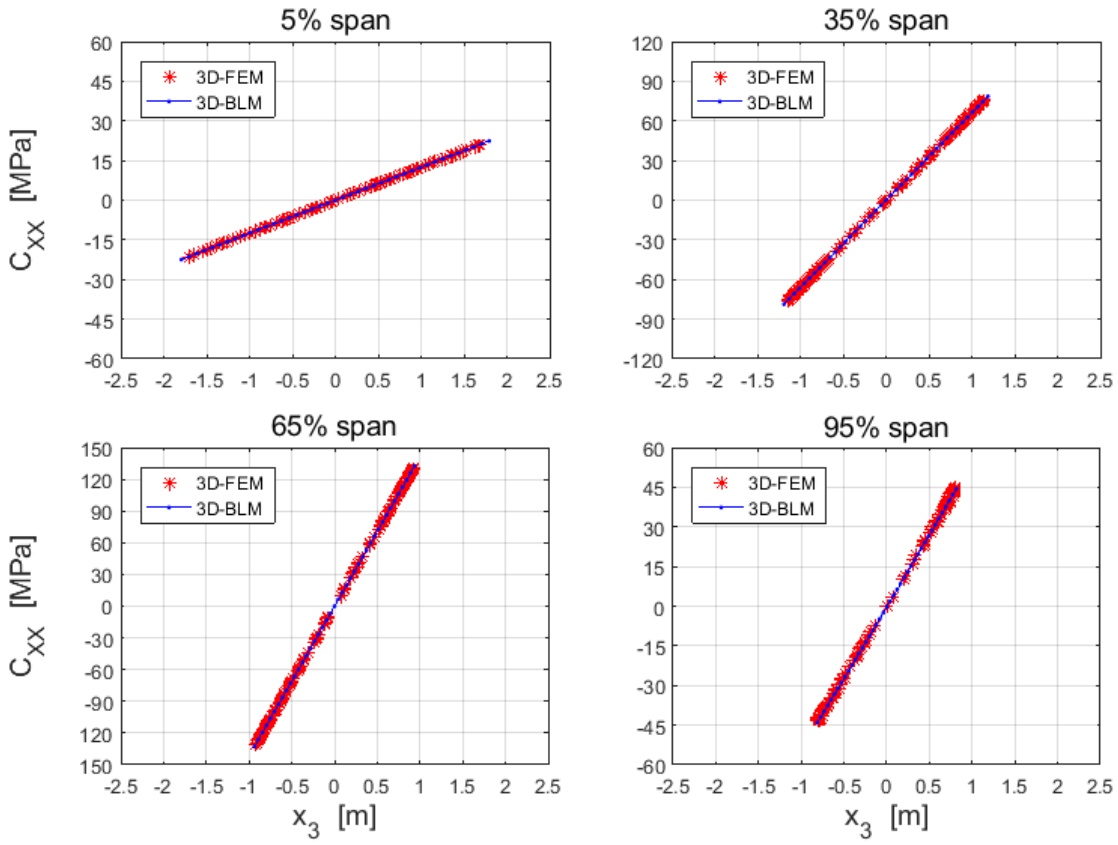

Figure 24: Longitudinal normal stress C_{XX} in the cross-sections at 5%, 35%, 65%, 95% span for F = 1000 kN

The results of the case studies addressed so far show that the model and formulas presented in this work are in close agreement with the results of nonlinear 3D-FEM and that they could be effectively used in predicting the mechanical response of bi-tapered beams even when the current and reference states of such beams cannot be assumed to almost coincide.

6 CONCLUSIONS

The stress fields in tapered beams cannot be properly predicted via the methods and formulas (e.g., Jourawski's) commonly used for prismatic beams: the spanwise variation of their cross-sections produces non-trivial stress distributions absent in prismatic elements. Additional difficulties arise in the event of large displacements, which further complicate the derivation of closed-form formulas for engineering applications.

By exploiting the results of previous works, in the present paper we have proposed a new formula for evaluating the shear flow through the cross-sectional chords of bi-tapered beams, extending Jourawski's formula to bi-tapered beamlike elements susceptible to large deflections and small strains.

Example applications have been presented and discussed; they address two tapered beams with rectangular and elliptical cross-sections and different taper coefficients. In both cases the results obtained for the shear stresses have been compared with those of nonlinear 3D-FEM simulations and with some noteworthy results available in the literature. In particular, in the first case the comparisons have been made with the Jourawski's solution (applied to the tapered beam as if it were a stepped beam) and Bleich's solution, both based on the linear beam theory (the latter accounting for the effects of taper in variable depth beams). Specifically, we have shown how the proposed solution reduces to Bleich's (amongst others) if the actual and reference shapes of the beam are very close each other. In addition, we have also discussed how Jourawski's solution is re-obtained if the taper vanishes. In the second example an analytical solution has been used to assess the performance of the proposed shear formula. In all cases, the results obtained with our model (3D-BLM) and shear formula turned out to be in very good agreement with those of nonlinear 3D-FEM simulations.

The results and shear formula presented in this paper neglect the effects of some geometric characteristics (e.g. pre-twist) and material properties (e.g. non-homogeneity). The inclusion of additional terms associated with such geometric and material characteristics (along with those already accounting for the taper) may be important to accurately predict the stress and strain fields and obtain a more general shear formula for pre-twisted, tapered beams. These are important points for further investigation and will addressed in subsequent works.

APPENDIX

In the case of rectangular cross-sections, equations (34)-(39) generalize the Jourawski's solution for prismatic beams [5]. It is worth noting that if the current and reference states of the beam are very close and can be thought to almost coincide, such equations reduce to the formulas made available in the literature by other investigators who have studied the effects produced by the taper (e.g. [10,15,16]). To prove this, it is sufficient to specialize (37) for a flapwise linearly tapered beam, loaded at the tip by an axial force N, transverse force T, and bending moment M, undergoing small displacements of the centre-line and small rotations of the local triads. Starting with (37), with $\theta \simeq 0$, we obtain:

$$\frac{q}{2h_2} = \frac{(h_3^2 - x_3^2)}{2J_2} F_Z + \frac{\Lambda_3^{-1}\Lambda_3' x_3}{A} F_X + \frac{\Lambda_3^{-1}\Lambda_3'(3x_3^2 - h_3^2)}{2J_2} M_Y . \tag{46}$$

The next step is to express coefficient Λ_3 as a linear function of *s*:

$$\Lambda_3 = 1 - \frac{\tan\alpha}{h_{3R}} s\,, \tag{47}$$

where h_{3R} is the height of the cross-section at the root (i.e., at $s = 0$), and angle α denotes the slope of the beam extrados. Combining (46)-(47) yields

$$\frac{q}{2h_2} = \frac{(h_3^2 - x_3^2)}{2J_2} F_Z + \frac{x_3 \tan\alpha}{Ah_3} F_X + \frac{(3x_3^2 - h_3^2)\tan\alpha}{2J_2 h_3} M_Y \tag{48}$$

The expressions for the cross-sectional area A and moment of inertia J_3 for the present case are to be substituted into (48), as are those for the cross-section resultants F_X, F_Z, M_Y with those in terms of axial force N, transverse force T, and bending moment M applied at the tip section, i.e. $F_X=N$, $F_Z=T$, $M_Y=M-T(L-s)$, where L is the beam length. We finally obtain

$$\frac{q}{2h_2} = -\frac{3(x_3^2 - h_3^2)h_3 - 3(3x_3^2 - h_3^2)(L-s)\tan\alpha}{8h_2 h_3^4} T - \frac{x_3 \tan\alpha}{4h_2 h_3^2} N - \frac{3(3x_3^2 - h_3^2)\tan\alpha}{8h_2 h_3^4} M \tag{49}$$

which is the expression we can find, for example, in [16].

A similar relation can be obtained for elliptical cross-sections. As an example, still assuming small displacements, when one dimension, say h_2, is kept constant and a linear taper is assumed for the other, h_3, starting with (43), we get

$$\frac{q}{2d_2} = -\frac{4(x_3^2 - h_3^2)h_3 - 4(4x_3^2 - h_3^2)(L-s)\tan\alpha}{3\pi h_2 h_3^4} T - \frac{x_3 \tan\alpha}{\pi h_2 h_3^2} N - \frac{4(4x_3^2 - h_3^2)\tan\alpha}{3\pi h_2 h_3^4} M \tag{50}$$

Similar expressions can be obtained for other tapered beams, characterized by solid or hollow cross-sections of various shapes, and will be presented in subsequent works.

Compliance with Ethical Standards

Conflict of Interest: The authors declare that they have no conflict of interest.

REFERENCES

[1] Navier C.L.M.H., Résumé des leçons données à l'école des ponts et chaussées sur l'application de la mécanique a l'établissement des constructions et des machines, 3me éd., avec des notes étendues par M. Barré de Saint-Venant, Dunod, Paris, 1864.

[2] Love A.E.H., *A treatise on the mathematical theory of elasticity* 4th ed., Dover, NY, 1944.

[3] Sokolnikoff I.S., *Mathematical theory of elasticity* 1nd ed., McGraw-Hill, NY, 1946.

[4] Timoshenko S.P., Goodier J.N., *Theory of Elasticity* 2nd ed., McGraw-Hill, NY, 1951.

[5] Jourawski D.I., Sur la résistance d'un corps prismatique et d'une piéce composée en bois ou on tôle de fer à une force perpendiculaire à leur longeur. *Annales Des Ponts Et Chaussées* 12:328-351, 1856.

[6] Balduzzi G., Hochreiner G., Fussl J., Stress recovery from one dimensional models for tapered bi-symmetric thin-walled I beams: deficiencies in modern engineering tools, *Thin-Walled Structures*, 119, 934-945, 2017.

[7] Timoshenko S.P., Gere J.M., *Mechanics of Materials*, Brooks/Cole Engineering Division, 2nd ed., 1984.

[8] Migliaccio G., Ruta G., The influence of an initial twisting on tapered beams undergoing large displacements, *Meccanica*, 56(7), 1831-1845, 2021.

[9] Slocum S.E., A general formula for the shearing deflection of arbitrary cross-section, either variable or constant. *Journal of the Franklin Institute* 171(4):365-389, 1911.

[10] Bleich F., *Stahlhochbauten Bd. 1*, Springer, Berlin, 1932.

[11] Pugsley A.G., Weatherhead R.A., The shear stresses in tapered beams, *The Aeronautical Journal* 46:218-226, 1942.

[12] Saksena G.B., Shear stress in a tapering beam, *Aircraft Engineering and Aerospace Technology* 16(2):47-50, 1944.

[13] Krahula J.L., Shear formula for beams of variable cross section, *AIAA Journal* 13(10):1390-1391, 1975.

[14] Russo E.P., Garic G., Shear-stress distribution in symmetrically tapered cantilever beam, *Journal of Structural Engeneering* 118(11):3243-3249, 1992.

[15] Cortinez V.H., Shear-stress distribution in symmetrically tapered cantilever beam, *ASCE Journal of Structural Engineering* 120(2):676-678, 1994.

[16] Taglialegne L., Analytical study of stress fields in wind turbines, *PhD thesis*, Unviersity of Florence, 2018.

[17] Bertolini P, Eder M.A., et al., Stresses in constant tapered beams with thin-walled rectangular and circular cross sections, *Thin-Walled Structures*, 137, 527-540, 2019.

[18] Balduzzi G., Aminbaghai M., et al., Non-prismatic beams: A simple and effective Timoshenko-like model, *International Journal of Solid and Structures*, 90, 236-250, 2016.

[19] Hodges D.H., Ho J.C., Yu W., The effect of taper on section constants for in-plane deformation of an istotropic strip, *Journal of Mechanics of Material and Structures*, 3, 425-440, 2008.

[20] Hodges D.H., Rajagopal A., et al., Stress and strain recovery for the in-plane deformation of an isotropic tapered strip-beam, Journal of Mechanics of Material and Structures, 5, 963-975, 2010.

[21] Berdichevsky V.L., On the energy of an elastic rod, Journal of Applied Mathematics and Mechanics, 45, 518-529, 1981.

[22] Zappino E., Viglietti A., Carrera E., Analysis of tapered composite structures using a refined beam theory, *Composite structures*, 183, 42-52, 2018.

[23] Shin D., Choi S., et al., Finite element beam analysis of tapered thin-walled box beams, *Thin-Walled Structures*, 102, 206-214, 2016.

[24] Li G.Q., Li J.J., A tapered Timoshenko-Euler beam element for analysis of steel portal frames, *Journal of Constructional Steel Research*, 58, 1531-1544, 2002.

[25] Nagel G.M., Thambiratnam D.P., Computer simulation and energy absorption of tapered thin-walled rectangular tubes, *Thin-Walled Structures*, 43, 1225-1242, 2005.

[26] Paglietti A., Carta G., La favola del taglio efficace nella teoria delle travi di altezza variabile, *Proc. of AIMETA conference*, Brescia, Italy, 2007.

[27] Paglietti A., Carta G., Remarks on the current theory of shear strength of variable depth beams, *The open civil engineering journal* 3:28-33, 2009.

[28] Balduzzi G., Sacco E., et al., Non-prismatic thin-walled beams: critical issues and effective modelling. *Associazione Italiana Meccanica Teorica e Applicata (AIMETA)*, 301-308, 2017.

[29] Trahair N.S., Ansourian P., In-plane behaviour of web-tapered beams, *Engineering Structures*, 108, 47-52, 2016.

[30] Orr J.J., Ibell T.J., et al., Shear behaviour of non-prismatic steel reinforced concrete beams, *Engineering Structures*, 71, 48-59, 2014.

[31] Zhou M., Fu H., An L., Distribution and properties of shear stress in elastic beams with variable cross section: theoretical analysis and finite element modelling, *KSCE Journal of Civil Engineering*, 4, 1-15, 2020.

[32] Singer F.L., Strength of materials, 2nd ed., Harper and Row, New York, 1962.

[33] Mercuri V., Balduzzi G., et al., Structural analysis of non-prismatic beams: Critical issues, accurate stress recovery, and analytical definition of the finite element (FE) stiffness matrix. Engineering Structures, 213, 110252, 2020.

[34] Migliaccio G., Non-prismatic beamlike structures with 3D cross-sectional warping, in the proc. of 14th World Congress in Computational Mechanics (WCCM) & ECCOMAS congress 2020, Paris, France, 11-15 Jan. 2021.

[35] Gurtin M.E., *An introduction to continuum mechanics, Mathematics in science and engineering*, Academic Press, 1st ed., 1981.

[36] Ruta G., Pignataro M., Rizzi N., A direct one-dimensional beam model for the flexural-torsional buckling of thin-walled beams, Journal of Mechanics of materials and structures, 1, 1479-1496, 2006.

[37] Dell'Isola F., Bichara A., *Elementi di algebra tensoriale con applicazioni alla meccanica dei solidi*, 1 ed., Società Editrice Esculapio, Bologna, 2005.

[38] Courant R., Hilbert D., *Methods of mathematical physics*, Interscience Publisher, 1st ed., 1953.

[39] Madenci E., Guven I., *The finite element method and applications in engineering using Ansys*, 2nd ed., Springer, 2015.

[40] Migliaccio G., Ruta G., et al., Beam-like models for the analyses of curved, twisted and tapered horizontal-axis wind turbine (HAWT) blades undergoing large displacements, *Wind Energy Science,* 5, 685-698, 2020, https://doi.org/10.5194/wes-5-685-2020.

[41] Migliaccio G., Ruta G., Rotor blades as curved, twisted, and tapered beam-like structures subjected to large deflections, *Engineering Structures*, 2020.